CALCIUM SIGNALING AND DIFFERENT SECRETORY VESICLES IN CHROMAFFIN CELLS

E.A. LUKYANETZ

Bohomolets Institute of Physiology, Kyiv, Ukraine elena@biph.kiev.ua



Elena Lukyanetz, Senior scientific researcher, Group leader, Associated Professor, Bohomoletz Institute of Physiology, Department of general gysiology of nervous system, International Center of Molecular Physiology, Academy Sciences of Ukraine, Kyiv, Ukraine. 1985: Master Degree, Kyiv State University, Department of Biophysics, Biological Faculty, Kyiv, Ukraine,; Biophysics; 1989: PhD student, under the guidance of Professor P.G. Kostyuk, Bohomoletz Institute of Physiology, Department of General Physiology of Nervous System, Kyiv, Ukraine; 1993; Ph. Degree in Biophysics, 2006: Dr Sci Degree in Biophysics. Visiting Scientist in Max-Planck- Institute of Biophysical Chemistry, Gottingen, Germany, Department of Biophysics (Head Dept Prof. E. Neher); Visiting Scientist at Royal Free Hospital School of Medicine, University of London, London, United Kingdom, Department of Pharmacology (Head Dept. Prof. A. Dolphin); Visiting Scientist in Marine Biological Laboratory, Woods Hole, USA (Head Dept. Prof. G. Augustin). She received lots of different scientific grants and several academic and state awards. The scope of interests concerns with neurosciences (biophysics, neuroscience, electrophysiology, cell biology, molecular biology).

Introduction

Exocytosis is one of the main cellular processes which enables the cell to influence its environment. This mechanism underlies the intercellular communication in the nervous system via neurotransmitter release in synapses and thus is a basis for integrative function of the brain. The involvement of numerous intracellular molecules in secretory pathway has been already shown. However, a major intracellular stimulus for exocytotic proceeding in excitable cells is a rise of intracellular Ca²⁺ concentration (Ca_i). It has been previously shown that Ca²⁺-dependence of secretion has a two-step character, which can be explained by several models, viz. a "pools" model in chromaffin cells (1, 2) or a "prepared stage" model of secretion in nerve terminals (3). Recently the involvement of a protein kinase C mechanism into biphasic phenomenon has also been proposed (4). The "pools" model assumes the existence of three vesicular pools and vesicle "migration" from large reserve to a release-ready and then to secreted pools. The existence of large reserve and releaseready pools determines a two-step secretion with the third-

power Ca²⁺-dependence of the final secretory response. The "prepared stage" model describes two steps, namely a threshold phase being a preparative stage for secretion and a secretory phase itself. The preparative stage serves as Ca²⁺-dependent "priming" step of secretion. The "PKC model" explains the two phases of secretion by PKC-dependent and -independent processes depending on Cai. In this paper we propose a 'vesicular' mechanism which describes experimental data and implies significance of this phenomenon in the function of secretory cells.

Materials and methods

Cell culture. Chromaffin cells were prepared by enzymatic dissociation of bovine adrenal glands and maintained in tissue culture for 2-5 days. Then they were plated on poly-L-lysine-coated glass coverslips and maintained in Medium 199 supplemented with 10% fetal calf serum, 1% bovine serum albumin and 2 mM glutamine for cell culture; see (5) for more details. We did not separate adrenalineand noradrenaline-secreted cells.

Electrophysiological measurements. Cells were voltage clamped using the whole-cell patch-clamp technique (6). Whole-cell Ca21 currents were recorded at high time resolution with a computer-controlled patch-clamp amplifier EPC-9 and "Pulse" software (HEKA Electronic, Lambrecht, Germany). Standard bath solution contained in mM: NaCl, 140; KCl, 2.8; CaCl2, 2; MgCl2, 2, Hepes, 10; TEACl, 10; tetrodotoxin, 0.01; pH 7.2; bath solutions with high Ca21 concentration contained: NaCl, 40; CaCl2, 60; MgCl2, 2, Hepes, 10; TEACl, 40; tetrodotoxin, 0.01; pH 7.2. Protocol of experiments was as described previously (5). The intracellular solution contained in mM: CsCl, 64; Cs2SO4, 28; ATP, 2; MgCl2, 2; EGTA, 0.5; Hepes, 10; N-methyl-D-glucamin, 10; GTP, 0.3; pH 7.4. The osmolarity of the solutions was adjusted to 320 mOsM with glucose. All compounds were obtained from Sigma. All experiments were performed at room temperature (21-24 °C).

Capacitance measurements. To measure the secretion, we used a high-resolution measurement of membrane capacitance (Cm) (7). The measurements were realized in whole-cell experiments by applying a sine wave stimulus of a DC holding potential 270 mV with a software "Lock-in". A 1-kHz, 10 mV peak-to-peak sine wave was generated by an ITC-16 multichannel interface (Instrutech, Inc., NY) controlled by Mac computer. The sine generation as well as phase sensitive detection of Cm were fulfilled with the software 'Lock-in amplifier' controlled by "Pulse" software and EPC-9 amplifier (HEKA Electronics). Differences in Cm (Δ Cm) before and after a depolarizing pulse were estimated off-line (5, 8). Data were analyzed statistically using Origin 5.0, Microcal Inc. (U.S.A.). Data are given as mean 6 SE unless indicated otherwise.

Fluorescence measurements. Patch-clamp and capacitance records were combined with Fura-2 fluorescence measurements to allow simultaneous on-line monitoring of Ca21 currents, exocytosis and Fura-2 fluorescence signals to measure

Cai. 100 mM Fura-2 was loaded into the cells via patch pipets. Ca21 concentration calculated from the ratios of light emission produced by 360 and 390 nm wavelengths according to Grynkiewicz et al. (9) was displayed on-line using a system by Luigs and Neumann (Ratingen, Germany); see for more details (10).

Materials. Thermanox and Aklar were obtained from Nunc Inc. (U.S.A.); Araldite was from Fluka AG, Germany. All other chemicals were purchased from Sigma.

Results

Efficiency of Ca21 entry toilnduce the exocytosis depends on esting Cai

In our experiments, we used a high bath Ca²⁺ concentration (60 mM) to induce secretion by single depolarizations of 50 or 200 ms durations. At such concentration a maximum of current-voltage curve was located at 140 mV. Chromaffin cells were depolarized with the trains of depolarizing pulses to induce a wide range of secretory responses evoked by Ca²⁺ current (ICa). The membrane potential was held at 270 mV and the trains of depolarizations were started at a reference potential (140 mV) corresponding to the maximum of current-voltage relationship (I-V) for ICa followed by a series of depolarizations to different membrane potentials which activated ICa (210 to 160 mV). The reference potential was randomly repeated several times in the series the same protocol as described previously (5). The amount of Ca²⁺ ions entering *into* the cell during membrane depolarization was estimated as a Ca2+ charge (Q), the integral of ICa and Cai was directly measured by fura-2. Fig. 1 demonstrates typical records of Cai transients, membrane capacitance, Cm as well as ICa traces evoked by reference potential (V_{Ref} 5 140 mV) in the same chromaffin cell. Series conductance remained constant for all presented recordings.

As seen in Fig. 1, membrane depolarizations induced a rapid increase of Cm with a subsequent decline, which we attributed to endocytosis. Such 'reversible' Cm responses were observed in most of our experiments. As we described in our recent investigations, in the case of stable prepulse resting level of Cai, similar Q values induced similar changes in the membrane capacitance, Δ Cm (Fig. 2, b from (5)). On the contrary, an increase of resting Cai affected the secretory responses of the cell. Fig. 1 presents evidence that the value of DCm changes strongly depends on the resting level of Cai. Thus, despite even smaller values of the ICa peak due to its run-down (Fig. 1, Ca current traces 4-6), at higher resting Cai (right part of the Ca²⁺ trace), the Q-induced changes in Cm (Δ Cm) were significantly larger (right part of the Cm trace). Fig. 2, a presents an example of the dependence of Δ Cm changes evoked by reference potential (140 mV) on resting Ca measured in one of the cells. In these experiments, Q values induced by the reference potential were in the range of 30-70 pC.

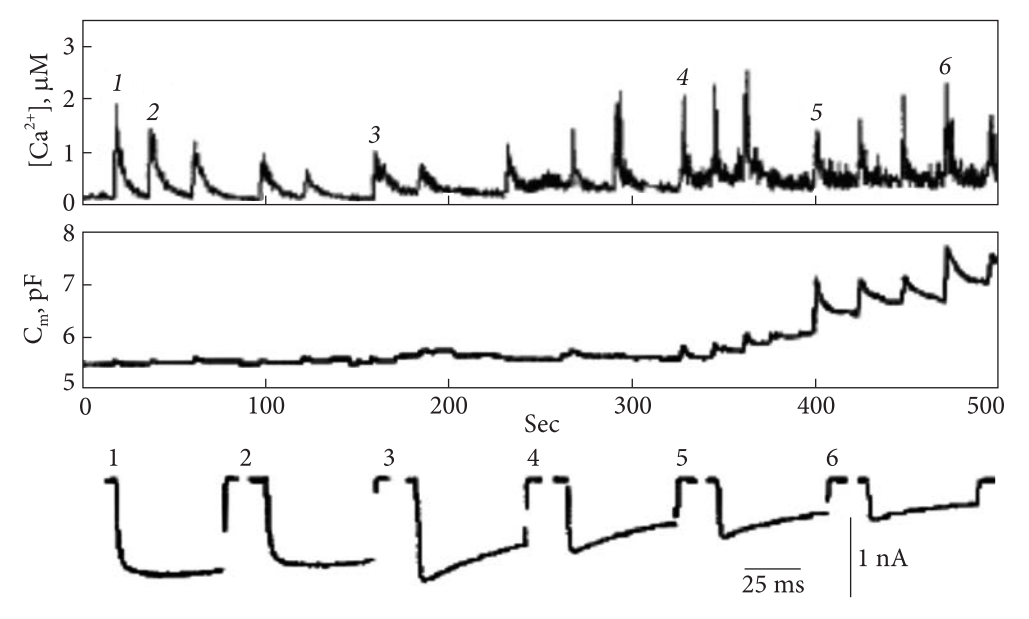


Fig. 1. Depolarization-induced exocytosis in bovine chromaffin cells. Changes in the intracellular Ca²⁺ concentration, Cai, membrane capacitance, Cm and Ca²⁺ current (ICa) traces induced by 50 ms depolarizations from a holding potential of 270 mV to different test potentials. Numbers pointed near Ca²⁺ current traces and Cai transients represent responses to reference potential (+40) which corresponds to a maximum of the current-voltage curve

The experimental points can be well approximated by the third-power calcium dependence curve (Fig. 2, a, solid line) as was supposed previously (1). Such a dependence was characteristic for all the tested cells (n = 47). Since the data recorded from different cells were scattered in absolute values, we analyzed one of the tested cells in detail. However, Fig. 2, a shows that the dependence of secretory response of the cell on Cai is composed of two parts. The first one represents slight dependence of DCm on Cai (similar to previously described 'preparative' step (3)). This step was observed when Cai changes were in the range below a critical level of Ca. (Ca*), which in our experiments was about 200÷300 nM for different tested cells. When Cai reached Ca*, Δ Cm evoked by the same Q was dramatically increased. Similar critical point (at Ca. ~300 nM) was also observed by the cited authors (3). Fig. 2, b demonstrates differences in mean values of Δ Cm induced by VRef measured at two different levels of resting Ca in the same cell. Thus, at low Cai ≤Ca*, the mean value of Δ Cm induced by Qref accounted for 72.78 \pm 18.97 fF (n = 6), and at high $Ca^* < Cai \le 600$ nM it was equal to 276.54 ± 134.8 fF, n = 5 in the same cell. We calculated these values as averaged within the corresponding range of Cai. Since in the range of high Cai the Δ Cm growth is considerable, significant deviations of Δ Cm values and low statistical significance (P < 0.2) were due to essential difference in Δ Cm laying in the poles of the range, see Fig. 2, a.

Two components of Ca²⁺-dependent secretion

Taking into account the observation described above, we estimated the influence of resting level of Cai on depolarization-induced secretion. DCm changes induced by Q were calculated separately for two levels of resting Cai, below and above the critical level Ca* = 250 nM. Fig. 2, c shows an example of Δ Cm dependence on Q recorded at low resting Cai \leq Ca* in the same cell. As seen, the experimental points can be well approximated by a linear graph with a slope of B1 = 4.43. Fig. 2, d demonstrates the dependence obtained for the same cell but at high level of resting, Cai

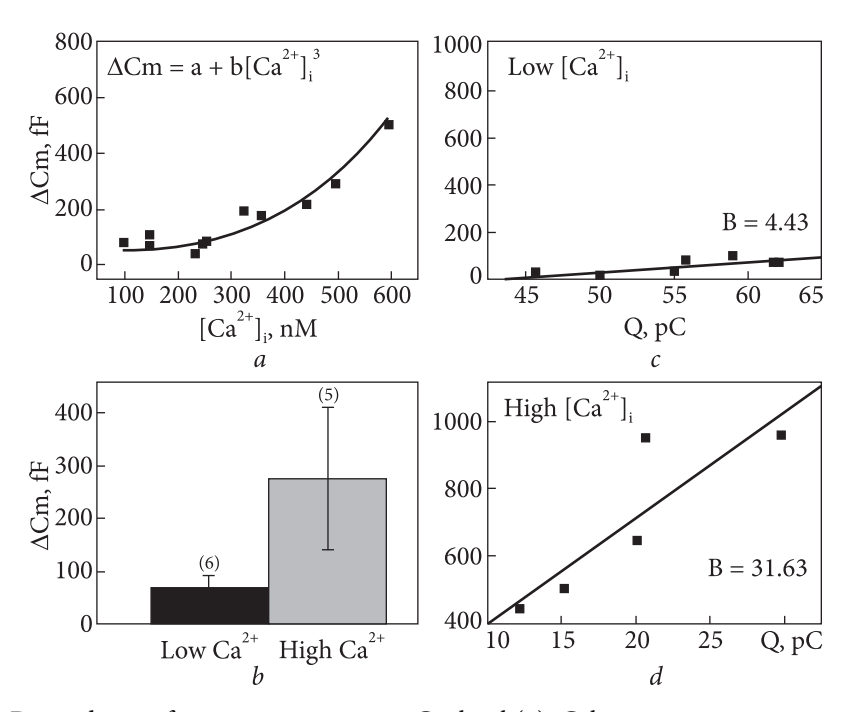


Fig. 2. Dependence of exocytosis on resting Cai level (*a*). Calcium concentration was measured using Fura-2 loaded into the cell by diffusion from the patch pipet solution (for more details see (5)). Experimental points represent DCm plotted against calcium concentration Cai recorded just before every depolarization in the same cell. ΔCm changes were induced by ICa with a Ca²+ charge lying in the range of 30-70 pQ. The equation DCm 5 aCai 3, where a is a proportionality constant (solid line), was fitted to the plot of DCm versus Cai; *b* — Representation of comparison of changes in DCm against the resting level of Cai for the same cell at low (Cai # 200 nM, black bar) and high (Cai > 200 nM, gray bar) resting Cai preceding depolarizing pulses. Error bars represent SD and numbers of tested values are presented near the bars. (*c*-*d*) Two components of exocytosis recorded at different resting Cai in bovine chromaffin cells; *c* — Linear increase in the value of ΔCm depending on Q value observed at low resting Cai ≤ 200 nM was well approximated by linear function with a slope B 5 4.43; *d* — Similar linear function with the slope B = 31.63 approximated data points obtained at Cai higher than 200 nM in the same cell

> Ca^* . In this case, the experimental points can also be approximated by a linear function, but the slope is obviously steeper ($B2^* = 31.63$).

Vesicular model of two-step Ca21-dependent secretion

Suppose two steps of secretion are triggered by different levels of resting Cai, then the simplest explanation for this could be the participation of two types of vesicles in the fusion process. If assume that at low level of Cai only small vesicles (SV) fused with the cell membrane, then this fusion would induce an insignificant increase in the cell membrane area proportionally to the vesicular surface area (S1) and the number (n1) of fused vesicles. It is generally accepted that the cell membrane capacitance, reflecting the cell membrane area, is usually calculated from the equation for a parallel plate capacitor. The changes in Cm (Δ Cm) produced by vesicle fusion are

$$\Delta C_{\rm m}(n_{\rm l}) = n_{\rm l} \frac{\varepsilon \varepsilon_{\rm 0} \cdot S_{\rm l}}{d},\tag{1}$$

where $\varepsilon_0 = 8.9 \cdot 10^{-12}$ F/m is the dielectric permeability in the vacuum, $\varepsilon = 3$, relative dielectric permeability, and d = 3 nm is the membrane thickness. If one takes into account that $\varepsilon \varepsilon \sigma \pi / d$ is a constant which equals to about 0.03 F/m² (30 fF/mm²), Eq. [1] can be easily transformed to a simpler expression

$$\Delta C_{m}(n_{1}) = 30n_{1}D_{1}^{2},\tag{2}$$

where D_1 is the diameter of SV taken in micrometers. The linear graph constructed from Eq. [2] is presented in Fig. 3, a (curve D_1) and looks like that describing the experimental points obtained at low Cai, Fig. 2, c.

(Ca*) large vesicles (LVs) start fusing with the membrane, then the function describing the fusion also will be linear but with a steeper slope (Fig. 3, a, line D_2) similar to the linear function describing experimental data (Fig. 2, d). For this case, the equation is as follows:

$$\Delta C_{\rm m}(n_2) = 30 n_2 D_2^2, \tag{3}$$

where n, is the number of fused LVs and D, is their diameter.

Obviously, due to the linearity of DCm(Q) obtained from experimental data (Fig. 2, c and d), it is reasonable to consider that the number of fused vesicles depends linearly on Q. Taking into account the fact that an increase of Cai due to Ca21 entering the cell during depolarization is proportional to Q (Fig. 2, a from (5)) and also considering Eqs. [2] and [3], the overall process of DCm dependence on Cai induced by similar Q will not be linear and will be described by conditional equation presented in Fig. 3, b (curves D_1 and D_2) where $Ca^* = 200$ nM, k1 and k2 are the proportionality coefficients. Thus, sup-

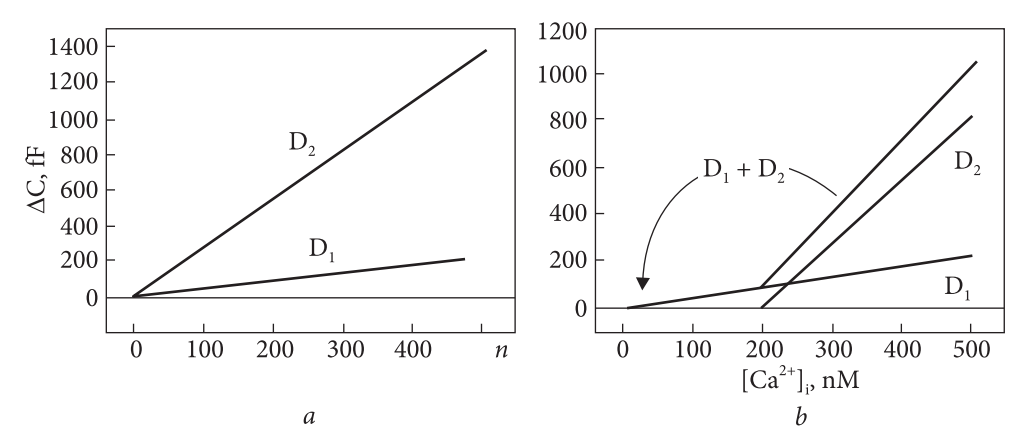


Fig. 3. Calculated dependence of exocytosis on the fusion of two types of vesicles: a — Simulation of changes in cell secretory response depending on the number (n) of fusing vesicles of two different diameters. Curve D_1 represents an increase of DCm due to fusion of small vesicles and curve D_2 describes fusion of large vesicles with the cell membrane; b — Summary solid line (D_1 1 D_2) describing the fusion of small (D_1) and large (D_2) vesicles in conditions when large vesicles start fusing after some delay determined by level of resting Cai. Corresponding separate graphs for D_1 and D_2 are presented by dotted straight lines. Start point of large vesicles fusion is determined by Cai level; 200 nM

pose the rate of fusion is constant, then the slope of linear functions *will reflect* the sizes of vesicles.

$$\Delta C_{\rm m}({\rm Ca_1}) = \begin{cases} 30k_1{\rm D_1^2~Ca_1}, & \text{for } {\rm Ca_1} \le {\rm Ca^*} \\ 30(k_1{\rm D_1^2} + k_1{\rm D_2^2}){\rm Ca_1}, & \text{for } {\rm Ca_1} > {\rm Ca^*}, \end{cases}$$
(4)

Assuming that at higher Cai the SVs continue to fuse with the membrane until their pool is emptied, the B^*2 slope will reflect the sum of two processes, the fusion of SVs and LVs ($B^*2 = B1 + B2$). From our experimental electrophysiological data (in accordance with the slopes), it can *be* as follows: (B1 + B2)/B1 = 7.14; consequently, the ratio of vesicular diameters is

$$\frac{\mathbf{D}_2}{\mathbf{D}_1} = 2.48 \cdot \sqrt{\frac{k_1}{k_2}}.\tag{5}$$

This means that the diameters of secretory vesicles participating in depolarization-induced exocytosis differ by about 2.5 times.

Discussion

We used electrophysiological measurements of calcium currents and membrane capacitance in combination with microfluorimetric measuring intracellular Ca²⁺ concentration to investigate the fine mechanisms of Ca²⁺-dependent secretion. Our experiments have shown two components of Ca²⁺-dependent exocytosis that

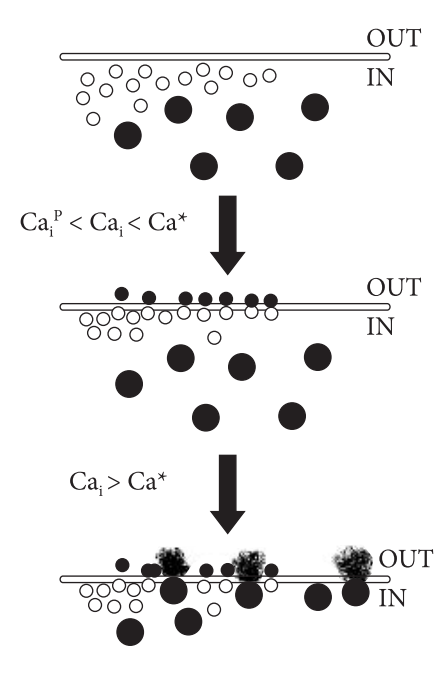


Fig. 4. Schematic representation of vesicular model. Small and large secretory vesicles are shown near the membrane. Abbreviations: Cai, cytoplasmic Ca²⁺ concentration; Cai*, critical point; Cai^p, physiological normal Ca²⁺ concentration

coincide with the data reported previously on chromaffin and other secretory cells (1-4, 11). We have established a linear dependence of both stages of exocytosis on Ca²⁺ influx during depolarization. Similar linear dependencies were also observed earlier, when the authors used EGTA buffers to fix Cai at two different levels (12). Here the data allow us to explain why a discrepancy between data describing DCm(Cai) dependence (linear or nonlinear was reported) does exist in the literature (1-3, 12). Linear dependence will be observed in the case if resting Cai level is

stable during the experiment. If it is changed only in the range below a critical level (about 200-300 nM), then a linear function with a low grade slope can be observed. If stable Cai is above the critical level, the function will be represented also by a linear graph with a sharper slope. Linear dependence will also be observed when resting Cai level passes both ranges, but if DCm is normalized to the reference values of the series. On the other hand, if resting level of Cai passes both ranges during experiment, then DCm(Cai) will correspond to the sum of two linear graphs and will look like an exponential-like dependence (Figs 2, *a* and 3, *b*).

Finally, we have presented a simple explanation of a two-step relationship between Cai and exocytosis, which is schematically presented in Fig. 4. The proposed 'vesicular' model consists in assumption that every phase of two-step secretion linearly depends on Cai and is provided by fusion of two different sized vesicles. According to presented data, the level of basal Cai determines which of the vesicular types starts to fuse. At slight increase of Cai which does not exceed the critical resting level (Cai < 200÷300 nM), fusion of small vesicles starts. Vesicles that have been filled with neurotransmitter translocate to the active zone by diffusion or by a cytoskeleton-based transport process where they dock and fuse with the plasma membrane. When Cai reaches the critical point, the larger vesicles start to fuse with plasmatic membrane. This process can provide very important physiological process — to trigger a release of different neurotransmitters which can be differently distributed among diverse secretory vesicles. For example, classical neurotransmitters located in synaptic-like microvesicles and peptide transmitters located in large dense core vesicles. Taking into account the fact that

chromaffin cells contain several types of secretory vesicles which are quite heterogeneous in their diameters (13-15), it is important to find types participating in exocytosis evoked by depolarization-induced increase of Cai.

Acknowledgements. We should like to thank sincerely Prof. P. Kostiuk and Prof. E. Neher. This work was supported by grants from the U.S. Civilian Research and Development Foundation for the Independent States of the Former Soviet Union (UB2-2049). This work was previously published (Lukyanetz, 2001).

REFERENCES

- Heinemann, C., von Ruden, L., Chow, R. H., and Neher, E. (1993) A two-step model of secretion control in neuroendocrine cells. *Pflugers Arch.* **424**, 105-112.
- Neher, E., and Zucker, R. S. (1993) Multiple calcium-dependent processes related to secretion in bovine chromaffin cells. *Neuron* **10**, 21-30.
- Seward, E. P., Chernevskaya, N. I., and Nowycky, M. C. (1995) Exocytosis in peptidergic nerve terminals exhibits two calciumsensitive phases during pulsatile calcium entry. *J. Neurosci.* **15**, 3390-3399.
- Smith, C., Moser, T., Xu, T., and Neher, E. (1998) Cytosolic Ca21 acts by two separate pathways to modulate the supply of release-competent vesicles in chromaffin cells. *Neuron* **20**, 1243-1253.
- Lukyanetz, E. A., and Neher, E. (1999) Different types of calcium channels and secretion from bovine chromaffin cells. *Eur. J. Neurosci.* 11, 2865-2873.
- Lukyanetz EA (2001) Different secretory vesicles can be involved in depolarization-evoked exocytosis. Biochemical and Biophysical Research Communications 288: 844-848.
- Hamill, O. P., Marty, A., Neher, E., Sakmann, B., and Sigworth, F. J. (1981) Improved patch-clamp techniques for high-resolution current recording from cells and cell-free membrane patches. *Pflugers Arch.* **391**, 85-100.
- Lindau, M., and Neher, E. (1988) Patch-clamp techniques for time-resolved capacitance measurements in single cells. *Pflugers Arch.* **411**, 137-146.
- Neher, E., and Marty, A. (1982) Discrete changes of cell membrane capacitance observed under conditions of enhanced secretion in bovine adrenal chromaffin cells. *Proc. Natl. Acad. Sci. USA* **79**, 6712-6716.
- Grynkiewicz, G., Poenie, M., and Tsien, R. Y. (1985) A new generation of Ca21 indicators with greatly improved fluorescence properties. *J. Biol. Chem.* **260**, 3440-3450.
- Neher, E. (1989) *in* Neuromuscular Junction (Sellin, L. C., Libelius, R., and Thesleff, S., Eds.), pp. 65–76. Elsevier, Amsterdam.
- Kirillova, J., Thomas, P., and Almers, W. (1993) Two independently regulated secretory pathways in mast cells. *J. Physiol. (Paris)* **87**, 203-208.
- Kim, S. J., Lim, W., and Kim, J. (1995) Contribution of L- and N-type calcium currents to exocytosis in rat adrenal medullary chromaffin cells. *Brain Res.* **675**, 289-296.
- Unsicker, K., and Chamley, J. H. (1977) Growth characteristics of postnatal rat adrenal medulla in culture. A study correlating phase contrast, microcinematographic, histochemical, and electron microscopical observations. *Cell Tissue Res.* **177**, 247-268.
- Koval, L. M., Yavorskaya, E. N., and Lukyanetz, E. A. (2000) Ultrastructural features of medullary chromaffin cell cultures. *Neuroscience* **96**, 639-649.
- Koval, L. M., Yavorskaya, E. N., and Lukyanetz, E. A. (2001) Electron microscopic evidence for multiple types of secretory vesicles in bovine chromaffin cells. *Gen. Comp. Endocrinol* **121**, 261-277.